Proceedings of the IASS 2024 Symposium
Redefining the Art of Structural Design
August 26-30, 2024, Zurich Switzerland
Philippe Block, Giulia Boller, Catherine DeWolf,
Jacqueline Pauli, Walter Kaufmann (eds.)

Structural form-finding, design and analysis of a freeform concrete shell for a gas station canopy

Qingpeng LI*, Qijian WU[a], Yao YE[a], Zai WANG[a]

*School of Architecture, Tianjin University
liqingpeng0318@163.com

[a] China Architecture Design & Research Group

Abstract

Structural form-finding, design and analysis of a freeform shell structure for a gas station canopy are carried out in this paper. Comprised of five interconnected sub-shells, the shell's horizontal projection is a right-angled trapezoid like shape, whose span is 72.5 meters. There are six arch-ribs within the shell structure, whose lateral projections should coincide. And lateral projections of upper contours of the five sub-shells should also coincide. Moreover, transverse cross-section of each sub-shell should be the same with each other. All these requirements from the architectural shape have brought rigorous constraints to the form-finding process. And then an improved form-finding and form-control process is addressed, and the stress ratio is introduced to assess its shell behavior. Subsequently, detailed structural design and analysis procedures are carried out to ensure the safety and integrity of the shell structure.

Keywords: freeform shell; structural form-finding; structural design; structural analysis

1. Introduction

Shown in Figure 1, the shell structure to be focused on in this article is the canopy structure of a gas station, part of the Xining Shuangzhai International Logistics City project, located in the eastern part of Duoba New City, Xining, Qinghai Province, China. The shell has a building projection area of approximately 2954 square meters and a longitudinal span of approximately 72.5 meters. The architectural design is inspired by the logo of the China National Petroleum Corporation and marine organisms such as shells closely related to petroleum, shown in Figure 2. At the same time, in response to the structural form requirements, multiple shell combinations are adopted to form a wavy shell with large rigidity and high bearing capacity, making the buildings in the entire site unified and diverse.

Currently, detailed design of the shell structure has been completed and is in the pending construction phase. And form-finding, design and analysis of this shell structure were carried out by the authors.

Figure 1: Architectural renderings of the freeform shell structure

Figure 2: Logo of the China National Petroleum Corporation and sea shells

2. Structural form-finding of the shell structure

It is well known that shell structures generated from hanging models have structurally efficient forms. Structural form finding of this project is based on this fundamental principle. However, due to the requirements of architectural aesthetics, there are several constraints in the form finding of the shell structure. Shown in Figure 3, these constraints primarily include: 1) Each sub-shell structure should have the same height for both its upper and lower edges when viewed from the south and north elevations of the building; 2) When viewed from the east-west sectional drawings of the building, the curvature and thickness variations of each sub-shell structure should also be consistent.

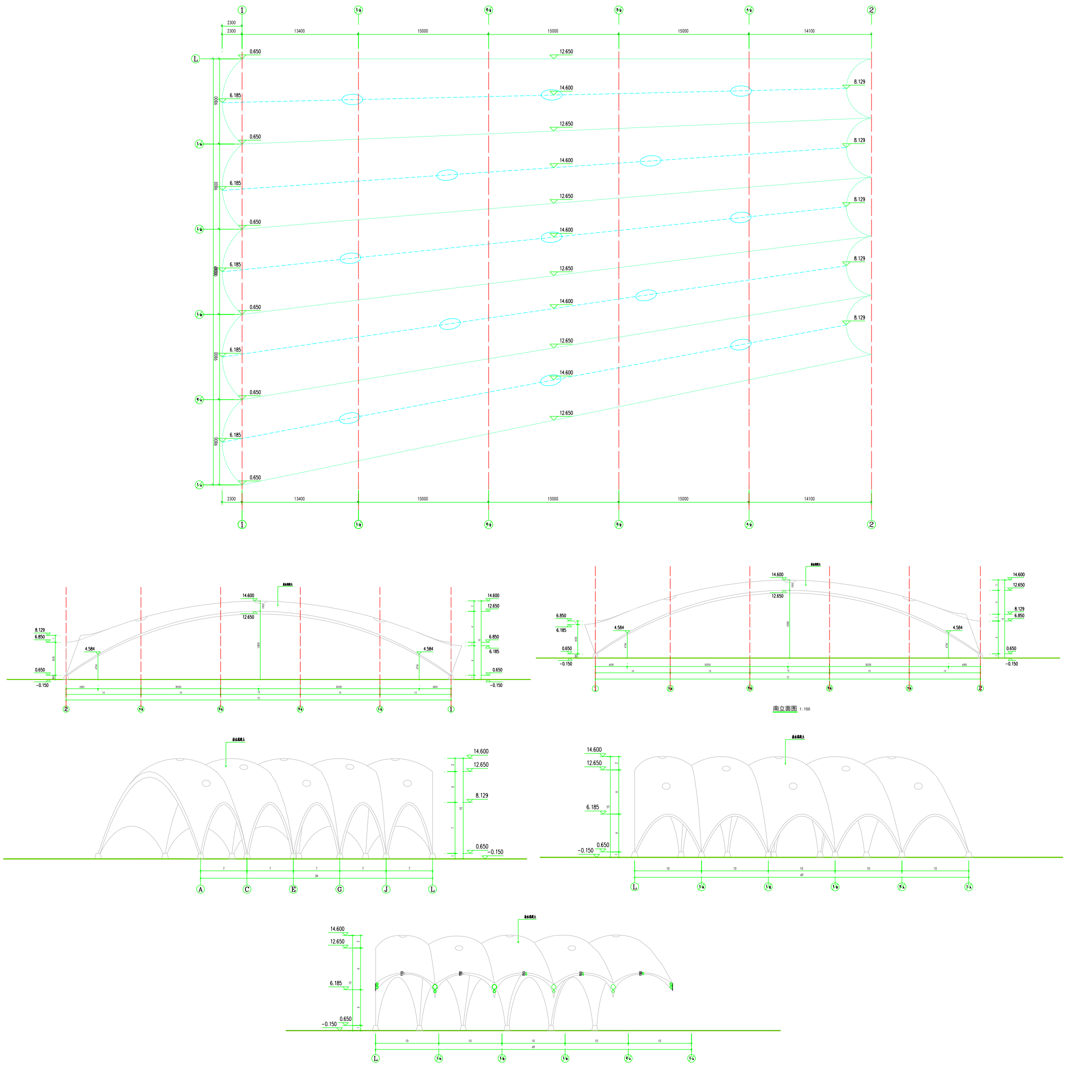

Figure 3: Architectural plan, elevations from four directions, and the east-west sectional drawing

To deal with these rigorous constraints, the structural form-finding process is as follows:

1) Establish an initial planar grid composed of parallelograms, shown in Figure 4. Identify the lines where the arch ribs are located, and determine the vertical load values at each point based on the associated surface area of each point.

2) Constrain 12 support points, restrain the lateral displacement of all points on the lines where the arch ribs are located, and use the force density method to determine the equilibrium shape of the planar cable net under vertical loading. Furthermore, utilize the inverse iteration method to adjust the force density of the line elements where the arch ribs are located to achieve the desired height of the arch ribs as per the architectural requirements.

3) Based on the form-finding results from the previous step, constrain the 12 support points and all points on the arch ribs. Then, adjust the force density of the grid lines in each sub-shell section to control the section height of each sub-shell. It is important to note that the elastic modulus of the grid lines in corresponding parts of all five sub-shells should be adjusted simultaneously to ensure consistency in the east-west sectional profiles of the five sub-shells.

Through the two rounds of form adjustment described above, a form-finding result has been obtained that meets the requirements of the architect and exhibits reasonably good structural performance, shown in Figure 5.

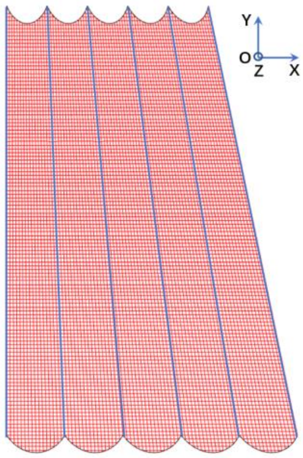

Figure 4: The initial planar grid

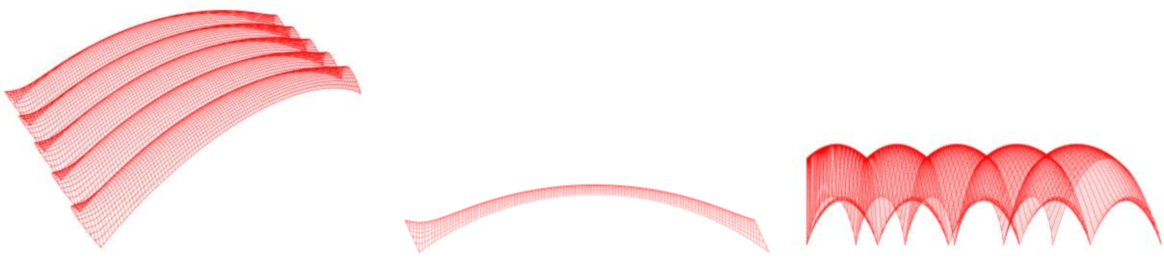

Figure 5: The form-finding result

Based on the form-finding results, establish a finite element model of the shell structure, shown in Figure 6, initially considering the distribution of shell thickness. Provide the arch ribs with greater bending stiffness to partially counteract the influence of restricting lateral displacement of the arch ribs during the form-finding process, especially for the two arch ribs at the edges. Subsequently, calculate the stress ratio of the shell structure to validate the rationality of the form-finding results [1]. Figure 6 shows a superior shell behavior in most part of the shell structure, while some bending moments occur near the edges that will be dealt with in the structural design process.

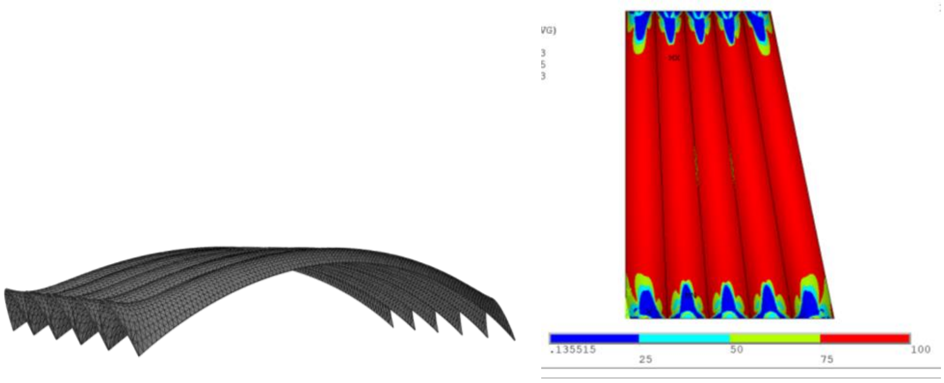

Figure 6: The finite element model of the shell and its stress ratio

3. Structural design of the shell structure

During the structural design phase, it is essential to address material selection, reinforcement, thickness design, and foundation design for the shell structure to ensure its structural safety under various loading conditions. Special attention should be given to designing the arch ribs, using thickness or structural stiffness control to mitigate the unreasonable shell behavior observed in the form-finding process. Under the guidance of multiple Chinese standards (some directly related ones are [2][3][4][5]), the structural design is completed through multiple iterative calculations, shown in Figure 7.

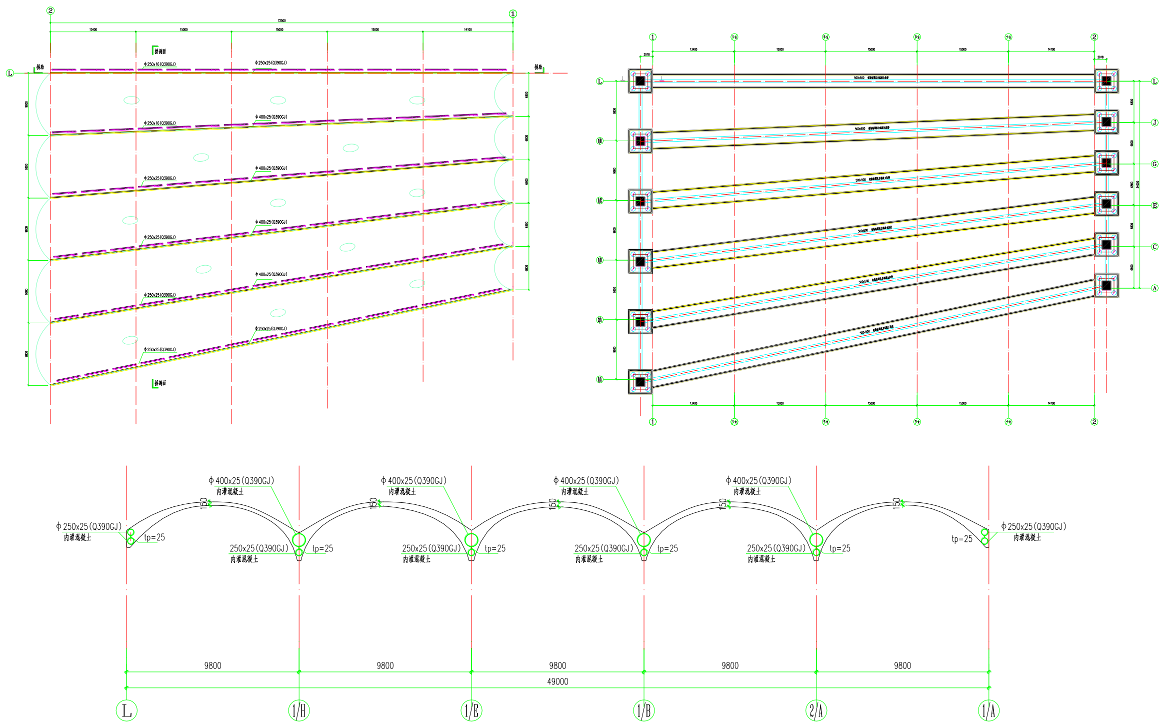

Figure 7: Structural plan, foundation plan, and structural sectional drawing

C50 concrete is used for the shell and the ground beam, and C30 concrete is used for isolated foundations, pedestals and pile foundations. HPB300 and HRB 400 are used for reinforcement. It should be noted that the thin-shell structure is reinforced with two layers of steel bars, so the minimum thickness of the shell is 15cm. Concrete filled steel tubular structures are used for the arch ribs. This is highly necessary for two reasons: firstly, in the form-finding process, the arch rib portion restricts lateral displacement, thus, the actual arch ribs must be able to withstand lateral forces; secondly, the stiff arch ribs provide a safer load transfer path for this structure and second line of defense. Moreover, between the two supports of the arch ribs, a ground beam is connected to resist the lateral thrust of the arch ribs.

4. Structural analysis of the shell structure

The safety of this shell structure under various loads has been validated during the structural design stage. However, the stability and seismic performance of the shell structure require special attention. This chapter introduces the results of nonlinear stability analysis and seismic analysis of this shell structure. To conduct these analyses, a detailed finite element analysis model based on ABAQUS 6.11 was established. The thin shell portion of the model was simulated using B3 shell elements (reinforced concrete thin shells simulated through layered shell elements), while the arch rib portion was simulated using B31 beam elements. Layered shell elements consist of a concrete layer in the middle and two layers of steel reinforcement mesh on the top and bottom, and dumbbell-shaped steel sections were used for the embedded steel bones at the arch ribs, shown in Figure 8. In the simulation analysis, steel and reinforcement materials were considered using a bilinear elastic-plastic model, while concrete materials were considered using the Concrete Damaged Plasticity (CDP) model, which accounts for tensile and compressive damage. The boundary conditions of the canopy structure model were fixed hinges at the arch feet.

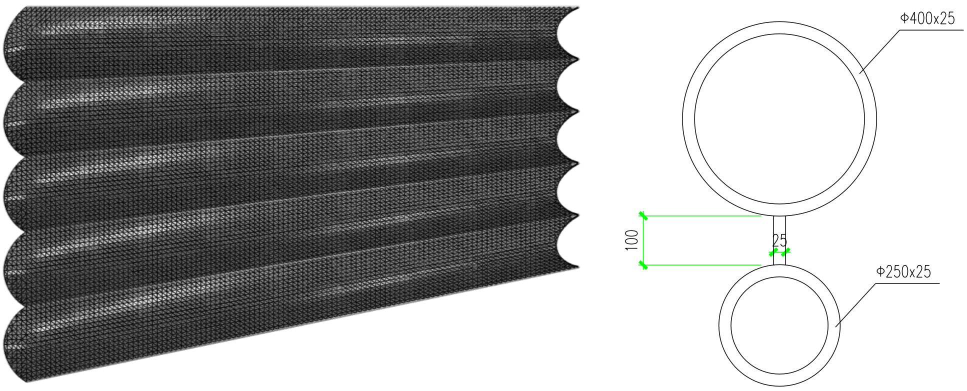

Figure 8: The finite element model and cross-section of the arch rib

4.1. Nonlinear stability analysis of the shell structure

A buckling modal analysis was conducted on the model, with a full-span load applied, equivalent to one times the standard load value (standard values for dead load plus live load). It was found that the first mode eigenvalue is 14.72 times the standard load value, shown in Figure 9, indicating that the model primarily experiences strength failure. Additionally, in subsequent elastic-plastic capacity analysis, initial geometric imperfections were introduced to the canopy structure in the form of the first buckling mode, with imperfections reaching a maximum of 1/300 of the span.

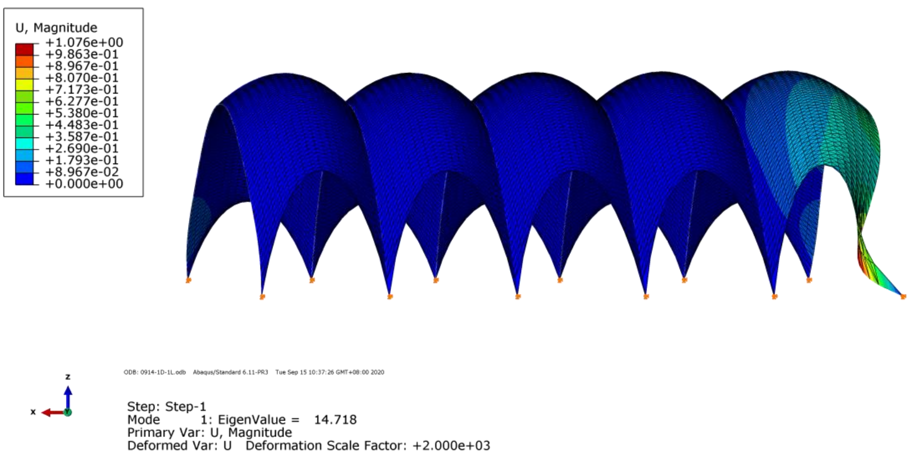

Figure 9: The first mode eigenvalue buckling mode

Through the nonlinear elastic-plastic analysis of the entire process of this shell structure, it is revealed that the canopy model reaches the ultimate limit state under a load of 7.66 times (standard dead load + full-span standard live load). At this point, the maximum deformation of the model occurs at the midsection of the edge ribs, with a maximum vertical deformation of approximately 136 to 308 mm in the inner shell. Extensive cracking occurs in the concrete core layer, with localized crushing at the arch feet, and partial plastic deformation of reinforcing bars (the bottom reinforcement layer at the end of the edge arch shell and at each arch foot enters plasticity and reaches ultimate strength at the arch foot; the top steel bars reach ultimate strength at the arch foot). Embedded steel bones at the arch ribs enter plasticity at each arch foot, shown in Figure 10.

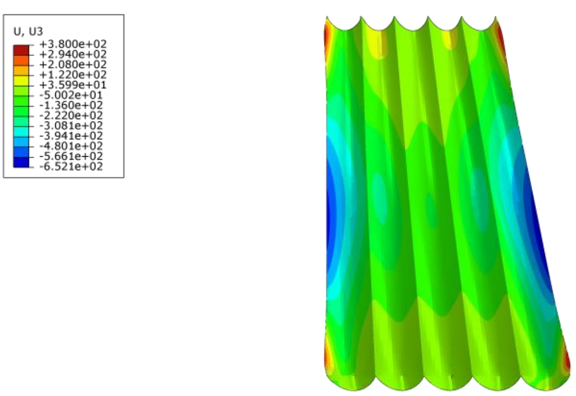

(a) Contour plot of the vertical deformation

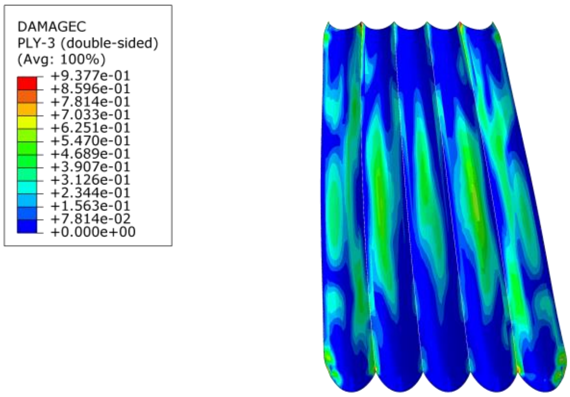

(b) Contour plot of compressive damage of concrete

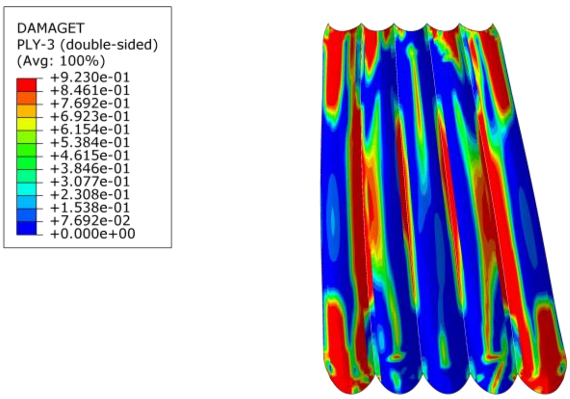

(c) Contour plot of tensile damage of concrete

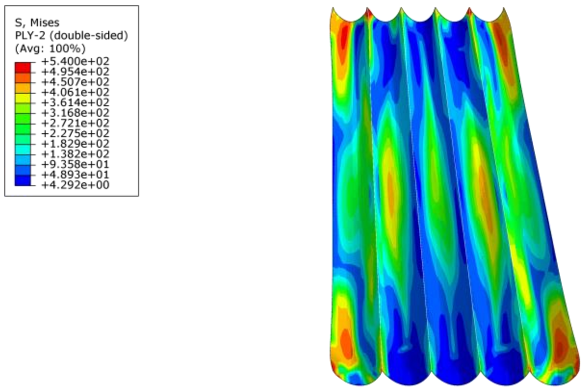

(d) Mises stress of bottom reinforcement layer

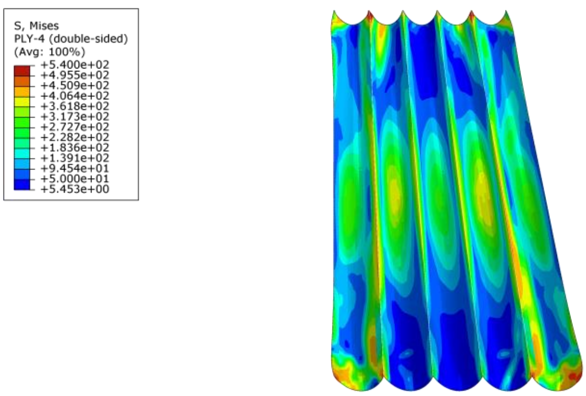

(e) Mises stress of top reinforcement layer

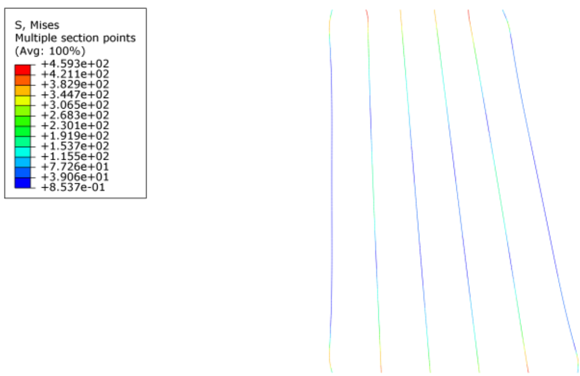

(f) Mises stress of arch rib embedded steel bones

Figure 10: Simulation results at the moment of concrete cracking

It can be observed that under vertical loading, the ultimate bearing capacity of the canopy structure model meets safety requirements. The maximum stresses in concrete and reinforcement (steel bones) occur at the column feet, which is characteristic of point-supported shells. To address this, a design measure involves increasing the wall thickness of the embedded steel bones at the column feet to ensure elasticity (excluding the contribution of external reinforcement concrete). Additionally, the lateral horizontal forces on the edge ribs are significant compared to the middle ribs (which can self-balance), resulting in higher maximum deformation and stress in the edge ribs. Therefore, reinforcement of the edge ribs is also necessary. By adding distributed reinforcement to localized areas according to stress distribution, the cracking load and ultimate bearing capacity can be further improved.

4.2. Seismic analysis of the shell structure

Using ABAQUS 6.11, seismic analysis is conducted on the finite element model of the canopy structure. Under the influence of artificial seismic records for a rare earthquake (Figure 11), elastic-plastic time history analysis was conducted using the time history analysis method for the structure.

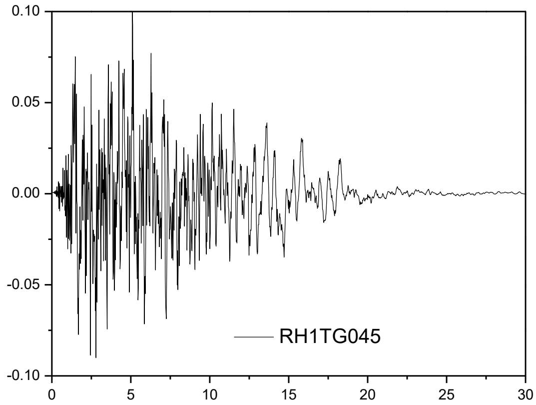

Figure 11: Artificial seismic records for a rare earthquake

Through analysis, shown in Figure 12, it can be observed that: 1) The concrete core layer of this structure exhibits severe damage. Concrete crushing is observed at the arch foot (compressive damage parameter greater than 0.9), and extensive tensile cracking is observed at both ends of the arch shell (tensile damage parameter greater than 0.9). 2) The stress level of the reinforcing steel in this structure is higher at the ends of the waveform shell. The maximum Mises stress of the bottom reinforcing steel is 362.8 MPa, and the maximum Mises stress of the top reinforcing steel is 344.2 MPa, both occurring in the arch foot region. 3) The embedded steel frames in the arch ribs of this structure remain elastic, but the stress level is relatively high (maximum Mises stress is 39.01 MPa).

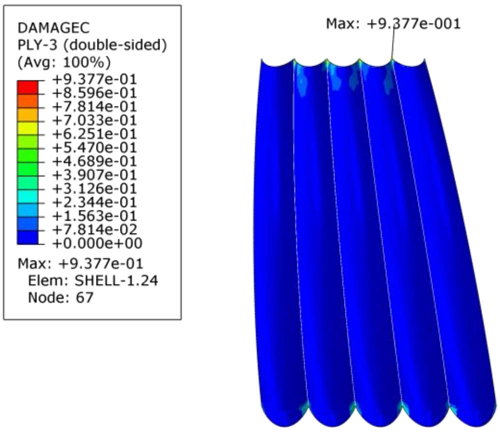

a) Contour plot of final compressive damage of concrete

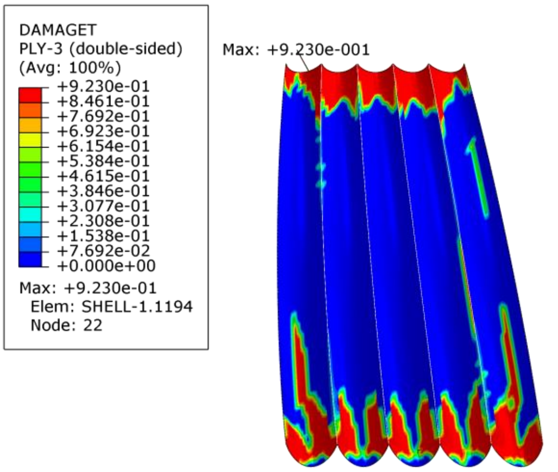

(b) Contour plot of final tensile damage of concrete

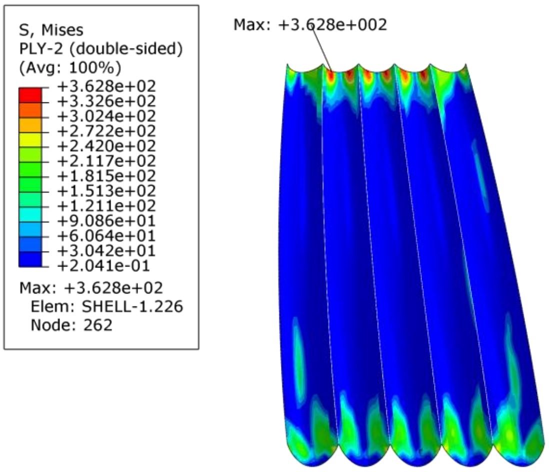

(c) Peak Mises stress of bottom reinforcement layer

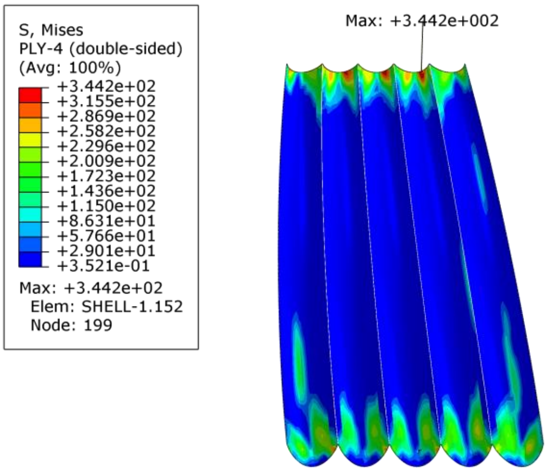

(d) Peak Mises stress of top reinforcement layer

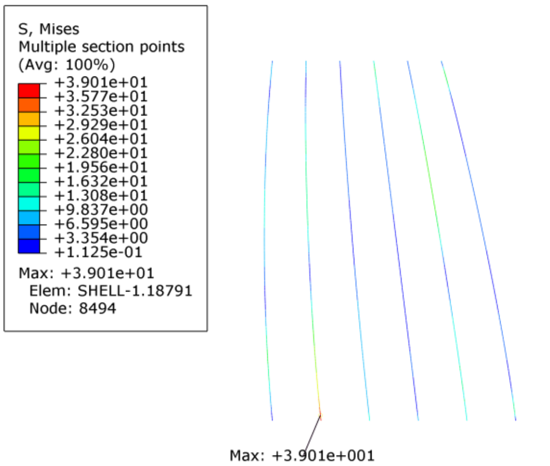

(e) Peak Mises stress of arch rib embedded steel bones

Figure 12: Results of rare earthquake time history analysis

Under the influence of a rare earthquake, this structure experiences significant concrete cracking. However, due to the presence of the arch ribs, the structure is ensured not to collapse. In fact, in the final seismic design of the structure, friction pendulum isolation bearings are installed at 12 supports, which significantly enhances the horizontal seismic performance of the canopy structure, which is not covered in this paper.

5. Conclusions

Shell structures derived from suspended models exhibit inherently efficient forms. Leveraging this principle, we engage in the structural form-finding of a freeform shell to adorn a gas station canopy. However, owing to the exacting demands of architectural aesthetics, we refine our form-finding and control procedures to adeptly address these challenges. Thus, the introduction of stress ratio assessment becomes pivotal in validating our form-finding outcomes. Following this, meticulous structural design ensues, encompassing material selection, thickness optimization, foundation planning, arch rib cross-section design, and beyond. Subsequent to this, nonlinear stability analysis is undertaken to ascertain its resistance against buckling, while seismic analysis ensures its robustness in the face of earthquakes, thereby ensuring utmost safety and structural integrity. Finally, based on the results of nonlinear stability analysis and seismic analysis, measures such as setting up seismic isolation friction bearings are employed to optimize the previous structural design.

References

[1] Q. Li, "Form Follows Force: A theoretical framework for Structural Morphology, and Form-Finding research on shell structures", PhD thesis, Delft University of Technology, 2018.

[2] GB50010-2010. Code for design of concrete structures. China.

[3] JGJ22-2012. Specification for design of reinforced concrete shell structures. China.

[4] GB50936-2014. Technical code for concrete filled steel tubular structures. China.

[5] GB50011-2010. Code for seismic design of buildings. China.

[6] ChatGPT.